ResearchGate

See discussions, stats, and author profiles for this publication at: https://www.researchgate.net/publication/231656093

Kinetic Study in a Microwave-Induced Plasma Afterglow of the Cu(2S) Atom Reaction with CH3Cl in the Temperature Range 389−853 K

ARTICLE *in* THE JOURNAL OF PHYSICAL CHEMISTRY · MAY 1996

Impact Factor: 2.78 · DOI: 10.1021/jp953204o

CITATIONS
2

READS
14

4 AUTHORS, INCLUDING:

Chris Vinckier
University of Leuven
118 PUBLICATIONS **1,453** CITATIONS
SEE PROFILE

Minh Tho Nguyen
University of Leuven
748 PUBLICATIONS **10,835** CITATIONS
SEE PROFILE

Available from: Chris Vinckier
Retrieved on: 23 January 2016

Kinetic Study in a Microwave-Induced Plasma Afterglow of the Cu(^{2}S) Atom Reaction with CH_3Cl in the Temperature Range 389−853 K

Chris Vinckier,* Inge Vanhees, Debasis Sengupta, and Minh Tho Nguyen

Department of Chemistry, University of Leuven, Celestijnenlaan 200F, B-3001 Leuven, Belgium

Received: October 30, 1995; In Final Form: February 9, 1996[⊗]

A kinetic study of the reaction $Cu + CH_3Cl \xrightarrow{k_1} CuCl + CH_3$ has been carried out in a fast-flow reactor. The gas phase copper atoms were generated using the microwave-induced plasma (MIP) afterglow technique. Atomic absorption spectroscopy at 327.4 nm was used as the detection technique. The influence of the experimental parameters such as the hydrogen content, sublimation temperature of CuCl pellet, and reactor pressure on k_1 has been verified. The rate constant k_1 was measured at temperatures between 389 and 853 K, which resulted in the Arrhenius expression $k_1 = (1.73 \pm 0.45) \times 10^{-11} \exp(-34.7 \pm 1.2 \text{ kJ mol}^{-1}/RT)$ cm^3 molecule^{-1} s^{-1}. Since the Arrhenius plot shows a slight curvature, the values of k_1 were also fitted to the modified Arrhenius equation $k(T) = AT^n \exp(-E/RT)$. Meaningful kinetic parameters can only be derived when n is fixed. A value of $n = 2.15$ was obtained using transition state theory combined with ab initio molecular orbital calculations. In that case the activation barrier of the reaction is lowered to 24.8 kJ mol^{-1}. The measured values of k_1 as a function of temperature can best be calculated over the 389−853 K range by the expression $\log k_1(T) = -21.22 - 10.99(\log T) + 3.30(\log T)^2$.

Introduction

The reactions of halomethanes with alkali-metal atoms have been investigated for more than 60 years. Already in the early 1930s Polanyi[1] and his collaborators studied reactions of alkali metals with several halogenated molecules in a diffusion flame. Numerous studies have been carried out using molecular beam techniques to determine the reaction cross sections. For the reactions with CH_3I the following cross sections were obtained:[2] 27 Å^2 (Li), 5 Å^2 (Na), and 35 Å^2 (K). The reactions of Na and K atoms with CH_3Br resulted in values of 6 and 3 Å^2, respectively.[3] These small reaction cross sections are an indication for a rebound mechanism for these alkali atom reactions.[4] In this case most of the alkali halide product recoils into the backward hemisphere with respect to the incoming alkali atom beam, which is in contrast to the stripping mechanism where most of the alkali halide recoils forward and the reactions have large cross sections (e.g., reactions with Br_2, ...). To explain the reactivity of Na atoms with halomethanes the electron-jump model was introduced.[4,5]

In addition to the measurements involving halogen molecules it appeared interesting to observe the effect of replacing a halogen atom by a less reactive methyl radical. Halomethanes are well suited for a systematic study such as testing the effect of electronegative substituents on reactivity.[6,7]

While the reaction of Cu atoms with Cl_2 has already been studied in our laboratory,[8] in the present work a kinetic study of the reaction between copper atoms and methyl chloride

$$Cu(4^2S) + CH_3Cl(^1A_1) \xrightarrow{k_1} CuCl(^1\Sigma^+) + CH_3(^2A''_2) \quad \Delta H_r = -17 \text{ kJ mol}^{-1} \quad (1)$$

was carried out in a fast-flow reactor. The microwave-induced plasma (MIP) afterglow technique was used as a source of the copper atoms in the gas phase.[9,10] The reaction was investigated in the temperature range from 389 to 853 K and the Arrhenius expression for k_1 has been derived. There are no other kinetic data on reaction 1 available in the literature but the rate constant could now be compared with the values calculated using the transition state theory, based on data obtained by ab initio MO calculations on the $Cu-CH_3Cl$ transition state structure.

Experimental Technique

As a detailed description of the experimental setup has been published previously,[11] only the essential characteristics of the technique will be repeated here. The $Cu + CH_3Cl$ reaction has been investigated in a quartz fast-flow reactor with an internal diameter of 5.7 cm and a length of 100 cm. At the upstream end, a sample holder carries a CuCl pellet. A Kanthal resistance wire allows to heat up this solid pellet up to a temperature T_s of about 800 K, independently of the temperature T_g in the reaction zone. The carrier gas argon transports the evaporated copper chloride oligomers $Cu_xCl_{x,g}$ downstream, where they are mixed with the reaction products of a hydrogen/argon MIP afterglow. In a complex and still unknown reaction sequence, hydrogen atoms convert a fraction of $Cu_xCl_{x,g}$ into Cu atoms.

In the kinetic zone, the copper atoms were detected by atomic absorption spectroscopy at 327.4 nm. The absorbances reached in the kinetic zone were of the order of 0.3 and lower, which correspond to an upper limit for the copper atom concentration of 4.3×10^{10} atoms cm^{-3}. Because of the much higher CH_3Cl concentrations, pseudo-first-order conditions for copper atom decays were fully established.

The temperature T_g in the kinetic zone of the reactor can be varied between 300 and 1000 K. The flow velocity v of the carrier gas argon is 324 ± 5 cm s^{-1} at 298 K. While the detection system remains at a fixed position, the fast-flow reactor assembly is mounted on a carriage which allows a horizontal displacement, so that copper absorbances can be measured along the reactor axis.

In the kinetic measurements several known amounts of CH_3Cl were added through the additive inlet and the decay of the copper atoms was followed as a function of the axial distance (z) and thus also of the reaction time $t = z/v$.

[⊗] Abstract published in *Advance ACS Abstracts,* April 15, 1996.

S0022-3654(95)03204-7 CCC: $12.00 © 1996 American Chemical Society

Gas flows were regulated by using Brook's precision needle valves of the ELF type or Brook's mass flow controllers, Model 5850 E.

The gases used were argon (5.0) from UCAR and CH_3Cl from Indugas with a purity better than 99.999 and 99.5%, respectively. Hydrogen is added as a 4.95% mixture in UHP helium (UCAR) or pure with a purity better than 99.9997% (L'Air Liquide).

Results and Discussion

Kinetic Expression for the Derivation of k_1. The rate constant of reaction 1 can be determined from the copper atom decays as a function of the reaction time at various amounts of CH_3Cl added. The formalism used for the derivation of k_1 is the same as in our previous work on the kinetics of copper,[10,11] sodium,[12] and magnesium[13,14] reactions:

$$\ln A_{Cu} = -\left\{\frac{k_1[CH_3Cl]}{\eta} + \frac{7.34D_{Cu,Ar}}{2r^2}\right\}t + B \qquad (2)$$

in which A_{Cu} is the copper absorbance, k_1 the rate constant of reaction 1, η a correction factor (depending on the flow characteristics), $D_{Cu,Ar}$ the binary diffusion coefficient of copper atoms in the carrier gas argon, r the reactor radius, t the reaction time ($=z/v$), and B an integration constant. While a complete discussion on the mathematics behind eq 2 is given by Howard et al.,[15] the influence of the various flow characteristics on the magnitude of η is discussed by Fontijn et al.[16]

The value of k_1 was determined by following first ln A_{Cu} as a function of the reaction time t at various amounts of CH_3Cl added. A weighted linear regression of ln A vs t was carried out using a statistical error for ln A that varies between 0.8 and 11.6% when going from the highest to the lowest value of ln A.

In the next step, the slopes S of these lines were plotted vs $[CH_3Cl]$. A weighted linear regression resulted in a straight line with an intercept of $7.34D_{Cu,Ar}/2r^2$ and a slope equal to k_1/η. For the measurements in argon the correction factor η was set equal to 1.3 with an associated systematic error of 10%. The uncertainties σ_S and σ_k for the calculated values of the slope S and the rate constant k_1 were calculated by combining the uncertainties of several variables like temperature, flow, reactor radius, and total pressure according to the method explained by Howard.[17] Finally, the systematic error of 10% for the correction factor 1.3 was taken into account resulting in the total standard deviation σ_k.

The plots and calculations were made by using the SAS-6.08 statistical package[18] available at our University Computer Centre.

This procedure is illustrated in Figure 1 where plots of the natural logarithm of the copper absorbance ln A_{Cu} as a function of the reaction time are shown for various amounts of CH_3Cl added. The experimental conditions were as follows: $T_g = 517$ K, the reactor pressure $P_r = 10$ Torr, and the MIP afterglow parameters T_s and $[H_2]$ respectively 509 K and 5.69 mTorr. When the slopes S of these lines are plotted vs the CH_3Cl concentration, a straight line is obtained as is shown in Figure 2. A weighted linear regression yields a value for $k_1 = (3.3 \pm 0.6) \times 10^{-15}$ cm^3 molecule^{-1} s^{-1} and an intercept I of 19.6 ± 0.4 s^{-1}.

The points shown at the ordinate are the observed copper decays in the blank experiments in the absence of the coreagent CH_3Cl. As an illustration, the lines for the experiments at two other temperatures are also shown in the same figure, giving

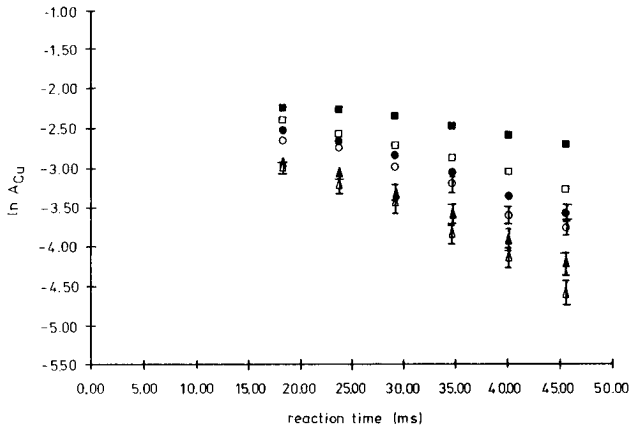

Figure 1. Natural logarithm of the Cu absorbance as a function of the reaction time. Experimental conditions: $T_g = 517$ K, $P_r = 10$ Torr, $T_s = 509$ K, $[H_2] = 5.69$ mTorr, $P_W = 40$ W, and the carrier gas is argon. The CH_3Cl concentrations are (■) 0, (□) 4, (●) 6.37, (○) 8.74, (▲) 11.3, (△) 13.9 in units of 10^{15} molecules cm^{-3}.

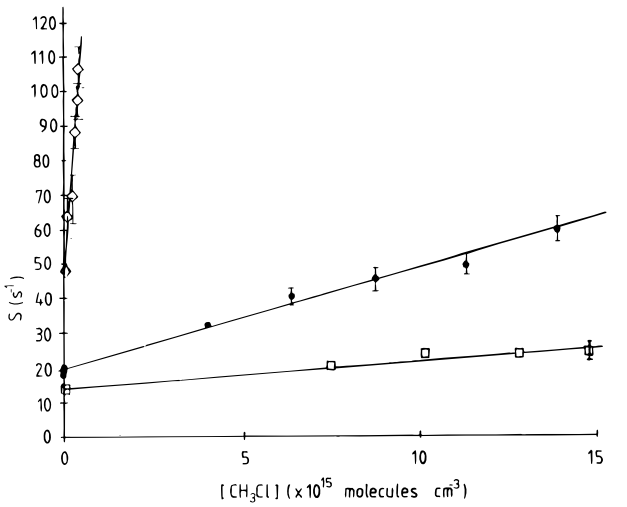

Figure 2. Observed slope, S, of eq 2 as a function of CH_3Cl concentration for three different temperatures: (□) 404 K, (●) 517 K, (◇) 757 K.

the values for $k_1 = (1.1 \pm 0.2) \times 10^{-15}$ and $(9.6 \pm 1.2) \times 10^{-14}$ cm^3 molecule^{-1} s^{-1} at, respectively, 404 and 757 K.

Influence of the MIP Afterglow Parameters. A number of MIP afterglow parameters have been varied to check whether or not they have an influence on the magnitude of the derived rate constants. An overview of the experimental conditions and results is given in Table 1. By changing the hydrogen content in the MIP afterglow, it was possible to check the influence of excess H atoms on the measured rate constant. Indeed they could react with a fraction of the added CH_3Cl or with CuCl to regenerate Cu atoms. Results in Table 1 show that there was no systematic effect of the hydrogen content on the derived value of k_1 at temperatures around 530 and 800 K. Hence, it seems reasonable to conclude that the interference of H atom reactions was negligible under these experimental conditions. When the microwave power P_W was varied between 20 and 70 W, also no effect was noticed on the value of k_1. Since increasing P_W resulted in higher MIP dissociation yields, this experiment confirmed the observation that the H atom concentration had no effect on k_1.

Since the sublimation of CuCl resulted in the formation of Cu_xCl_x oligomers,[19] a change of the sublimation temperature T_s from 519 to 544 K led to an increase of the gas phase concentration of the Cu_xCl_x oligomers by a factor of 4.4.[9] A

TABLE 1: Influence of the MIP Afterglow Parameters on the Value of k_1 for the Cu + CH_3Cl Reaction[a]

T_g (K)	T_s (K)	[H_2] (mTorr)	P_w (W)	P_r (Torr)	k_1 (cm^3 molecule^{-1} s^{-1})
		Hydrogen Content [H_2]			
528	535	2.12	40	10	$(4.8 \pm 0.9) \times 10^{-15}$
529	534	5.69	40	10	$(5.5 \pm 0.8) \times 10^{-15}$
530	536	52.58	40	10	$(5.6 \pm 0.9) \times 10^{-15}$
529	536	53.70	40	10	$(6.1 \pm 1.0) \times 10^{-15}$
532	536	136.23	40	10	$(5.8 \pm 1.0) \times 10^{-15}$
528	536	243.76	40	10	$(5.7 \pm 0.9) \times 10^{-15}$
800	537	19.53	40	10	$(1.5 \pm 0.2) \times 10^{-15}$
802	538	19.53	40	10	$(1.7 \pm 0.3) \times 10^{-15}$
810	540	41	40	10	$(1.5 \pm 0.3) \times 10^{-15}$
		Microwave Power P_W			
523	535	5.69	20	10	$(6.1 \pm 0.9) \times 10^{-15}$
528	535	5.69	40	10	$(6.3 \pm 1.2) \times 10^{-15}$
526	535	5.69	70	10	$(6.1 \pm 1.1) \times 10^{-15}$
		Temperature T_s of the Solid			
524	519	5.69	40	10	$(4.7 \pm 0.9) \times 10^{-15}$
521	533	5.69	40	10	$(4.4 \pm 0.8) \times 10^{-15}$
529	534	5.69	40	10	$(5.5 \pm 0.8) \times 10^{-15}$
525	536	5.69	40	10	$(3.9 \pm 0.7) \times 10^{-15}$
524	544	5.69	40	10	$(5.2 \pm 0.9) \times 10^{-15}$
		Reactor Pressure P_r			
529	528	19.53	40	6	$(7.7 \pm 1.4) \times 10^{-15}$
534	532	19.53	40	7	$(8.9 \pm 1.4) \times 10^{-15}$
526	534	19.53	40	8	$(7.2 \pm 1.0) \times 10^{-15}$
521	536	19.53	40	9	$(5.2 \pm 0.8) \times 10^{-15}$
525	536	19.53	40	10	$(6.3 \pm 1.0) \times 10^{-15}$
525	536	19.53	40	11	$(6.6 \pm 1.2) \times 10^{-15}$

[a] T_g, reaction temperature; T_s, temperature of the CuCl solid; [H_2], hydrogen content of the MIP; P_W, MIP power; P_r, reaction pressure.

variation of the temperature T_s of the CuCl pellet between 519 and 544 K does not show any systematic influence on the value of k_1.

Finally, when the reactor pressure was varied between 6 and 11 Torr, no effect on the value of k_1 could be observed, which confirms a second-order character for reaction 1. In addition, a lower reactor pressure enhances the diffusion of the reagents toward the reactor wall. The initial Cu absorbance for instance is a factor of 1.4 higher at 11 Torr than at 6 Torr. In view of the absence of a pressure effect on k_1, it can be concluded that neither the initial absorbances nor the hydrodynamic flow characteristics have any influence on the value of k_1.

Temperature Dependence of k_1. A summary of the experimental conditions and measured values of k_1 in the temperature range from 389 to 853 K is given in Table 2. A weighted nonlinear regression on these data results in the Arrhenius expression:

$$k_1 = (1.73 \pm 0.45) \times 10^{-11} \exp\left(\frac{-34.7 \pm 1.2 \text{ kJ mol}^{-1}}{RT}\right) \text{cm}^3 \text{ molecule}^{-1} \text{ s}^{-1} \quad (3)$$

The experimental results plotted as a conventional Arrhenius graph are shown in Figure 3. A weighted linear regression of ln k_1 vs $1/T$ yields the expression

$$k_1 = 1.76^{+0.40}_{-0.33} \times 10^{-11} \exp\left(\frac{-34.3 \pm 0.9 \text{ kJ mol}^{-1}}{RT}\right) \text{cm}^3 \text{ molecule}^{-1} \text{ s}^{-1} \quad (4)$$

It is obvious that both eqs 3 and 4 yield consistent Arrhenius parameters. In view of the symmetric error on the derived preexponential factor value, eq 3 will now be used further in the discussion. One might notice some deviation from linearity so that a non-Arrhenius behavior for reaction 1 might show up as will be discussed in the next section.

TABLE 2: k_1 of the Cu + CH_3Cl Reaction as a Function of Temperature[a]

T_g (K)	T_s (K)	[H_2] (mTorr)	P_W (W)	P_r (Torr)	k_1 (cm^3 molecule^{-1} s^{-1})
389	519	5.37	40	10	$(9.6 \pm 2.9) \times 10^{-16}$
397	520	5.37	40	10	$(8.2 \pm 2.2) \times 10^{-16}$
403	520	5.37	40	10	$(1.3 \pm 0.3) \times 10^{-15}$
403	534	4.39	40	10	$(9.8 \pm 3.6) \times 10^{-16}$
404	520	5.37	40	8	$(5.9 \pm 1.7) \times 10^{-16}$
404	520	5.37	40	9	$(1.1 \pm 0.2) \times 10^{-15}$
407	520	5.37	40	7	$(8.8 \pm 1.9) \times 10^{-16}$
417	521	5.37	40	10	$(1.3 \pm 0.3) \times 10^{-15}$
427	521	5.37	40	10	$(1.6 \pm 0.3) \times 10^{-15}$
432	532	4.88	40	10	$(1.9 \pm 0.5) \times 10^{-15}$
438	522	4.88	40	10	$(1.4 \pm 0.6) \times 10^{-15}$
452	518	5.37	40	10	$(1.8 \pm 0.3) \times 10^{-15}$
452	534	4.88	40	10	$(2.1 \pm 0.4) \times 10^{-15}$
456	527	4.88	40	10	$(2.3 \pm 0.9) \times 10^{-15}$
468	533	5.69	40	10	$(2.8 \pm 0.4) \times 10^{-15}$
476	520	5.53	40	10	$(2.8 \pm 0.4) \times 10^{-15}$
511	520	5.37	40	10	$(4.0 \pm 0.7) \times 10^{-15}$
514	522	5.69	40	10	$(3.5 \pm 0.7) \times 10^{-15}$
514	524	5.69	40	10	$(4.8 \pm 0.8) \times 10^{-15}$
515	520	5.69	40	10	$(4.3 \pm 0.8) \times 10^{-15}$
516	526	5.69	40	10	$(4.8 \pm 0.8) \times 10^{-15}$
517	509	5.69	40	10	$(3.3 \pm 0.6) \times 10^{-15}$
518	533	2.44	40	10	$(3.8 \pm 1.4) \times 10^{-15}$
520	517	5.69	40	10	$(6.5 \pm 0.8) \times 10^{-15}$
521	527	5.69	40	10	$(6.3 \pm 1.1) \times 10^{-15}$
521	533	5.69	40	10	$(4.4 \pm 1.7) \times 10^{-15}$
521	536	19.53	40	9	$(5.2 \pm 1.8) \times 10^{-15}$
523	534	5.69	40	10	$(5.6 \pm 2.0) \times 10^{-15}$
523	535	5.69	20	10	$(6.1 \pm 0.9) \times 10^{-15}$
524	519	5.69	40	10	$(4.7 \pm 1.8) \times 10^{-15}$
524	544	5.69	40	10	$(5.2 \pm 1.9) \times 10^{-15}$
525	518	5.69	40	10	$(5.8 \pm 0.9) \times 10^{-15}$
525	536	5.69	40	10	$(3.9 \pm 1.5) \times 10^{-15}$
525	536	19.53	40	10	$(6.3 \pm 1.0) \times 10^{-15}$
525	536	19.53	40	11	$(6.6 \pm 1.2) \times 10^{-15}$
526	534	19.53	40	8	$(7.2 \pm 1.0) \times 10^{-15}$
526	535	5.69	70	10	$(6.1 \pm 1.1) \times 10^{-15}$
528	535	2.12	40	10	$(4.8 \pm 1.9) \times 10^{-15}$
528	535	5.69	40	10	$(6.3 \pm 1.2) \times 10^{-15}$
528	536	157.82	40	10	$(5.7 \pm 2.0) \times 10^{-15}$
529	528	19.53	40	6	$(7.7 \pm 2.9) \times 10^{-15}$
529	534	5.69	40	10	$(5.5 \pm 1.9) \times 10^{-15}$
529	536	53.7	40	10	$(6.1 \pm 2.2) \times 10^{-15}$
530	536	19.53	40	10	$(6.9 \pm 1.0) \times 10^{-15}$
530	536	34.04	40	10	$(5.6 \pm 2.0) \times 10^{-15}$
532	536	88.2	40	10	$(5.8 \pm 2.2) \times 10^{-15}$
534	532	19.53	40	7	$(8.9 \pm 1.4) \times 10^{-15}$
553	521	5.69	40	10	$(9.1 \pm 1.2) \times 10^{-15}$
567	520	5.53	40	10	$(8.1 \pm 1.1) \times 10^{-15}$
600	533	5.69	40	10	$(1.3 \pm 0.2) \times 10^{-14}$
602	522	5.69	40	10	$(1.2 \pm 0.2) \times 10^{-14}$
643	532	21	40	10	$(2.6 \pm 0.4) \times 10^{-14}$
662	519	7.97	40	10	$(2.2 \pm 0.5) \times 10^{-14}$
692	544	20.2	40	10	$(5.0 \pm 0.7) \times 10^{-14}$
726	533	8.3	40	10	$(5.3 \pm 1.1) \times 10^{-14}$
757	532	11.39	40	10	$(9.6 \pm 1.2) \times 10^{-14}$
786	533	21.64	40	10	$(1.4 \pm 0.2) \times 10^{-13}$
800	537	19.53	40	10	$(1.5 \pm 0.2) \times 10^{-13}$
802	538	19.53	40	10	$(1.7 \pm 0.3) \times 10^{-13}$
810	540	41	40	10	$(1.5 \pm 0.3) \times 10^{-13}$
853	537	19.53	40	10	$(1.6 \pm 0.3) \times 10^{-13}$

[a] Symbols are the same as in Table 1.

No other kinetic data on reaction 1 have been reported in the literature yet. The reactions of CH_3Cl with alkali metal atoms have been studied,[20−23] but until now only Arrhenius expressions for Na[20] and K[21] have been derived in rather limited temperature

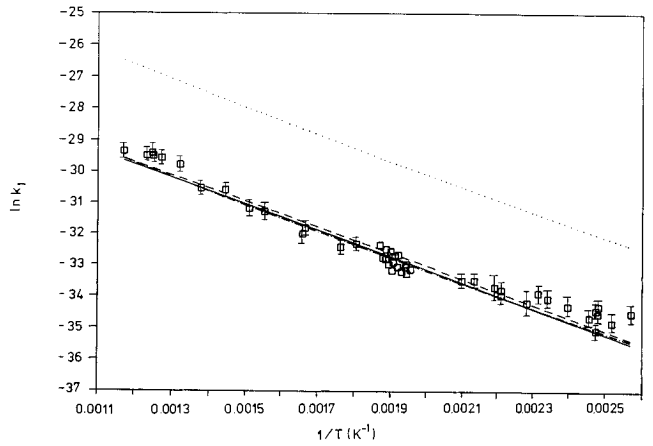

Figure 3. Arrhenius plot of ln k_1 vs $1/T$. Full line: nonlinear regression of k_1 vs $1/T$ described by eq 3; dashed line: linear regression of ln k_1 vs $1/T$ described by eq 4; dash dot line: nonlinear regression of k_1 vs T according to the three-parameter expression (7) with the value of n fixed at 2 (see Table 3); dotted line: k_1 calculated according to TST described by eq 12 and using data obtained by MO calculations.

ranges:

$$k_{Na+CH_3Cl} = 8^{+5}_{-3} \times 10^{-10} \exp\left(\frac{-44 \pm 4 \text{ kJ mol}^{-1}}{RT}\right) \text{cm}^3 \text{ molecule}^{-1} \text{ s}^{-1} \qquad 770-892 \text{ K} \tag{5}$$

$$k_{K+CH_3Cl} = 3.2^{+2.0}_{-1.2} \times 10^{-10} \exp\left(\frac{-32 \pm 3.6 \text{ kJ mol}^{-1}}{RT}\right) \text{cm}^3 \text{ molecule}^{-1} \text{ s}^{-1} \qquad 831-917 \text{ K} \tag{6}$$

To explain the reactivity of Na atoms with halomethanes, the electron-jump model was introduced.[4,5] Since the preexponential factor for Cu + CH_3Cl is of the order of 10^{-11} cm^3 molecule^{-1} s^{-1}, this harpooning mechanism could be ruled out. Nevertheless an "electron transfer" process might occur. In that case, the activation barrier could be interpreted as the energy required for transforming CH_3Cl into the anion CH_3Cl^-, which actually corresponds to the electron affinity of the neutral species. The potential energy curves of CH_3Cl and its negative ion have been calculated as a function of the C−Cl internuclear distance.[24] The energy difference between the intersection of the two potential curves and initial energy level of the molecule gives a value of 0.54 eV or 51.9 kJ mol^{-1} for the activation energy, which is larger than the experimentally determined activation energies of the Cu, Na, and K atom reactions.

Non-Arrhenius Behavior of the Cu + CH_3Cl Reaction. As mentioned before the Arrhenius plot in Figure 3 apparently exhibits a slight curvature. To describe this non-Arrhenius behavior, three-parameter expressions of the type

$$k(T) = AT^n \exp\left(\frac{-E}{RT}\right) \text{cm}^3 \text{ molecule}^{-1} \text{ s}^{-1} \tag{7}$$

are frequently used.

A weighted nonlinear regression for the values of k_1 in Table 2 leads to the modified Arrhenius equation

$$k_1 = (3.5 \pm 53.6) \times 10^{-15} T^{1.3\pm2.1} \exp\left(\frac{-32.6 \pm 10.6 \text{ kJ mol}^{-1}}{RT}\right) \text{cm}^3 \text{ molecule}^{-1} \text{ s}^{-1} \tag{8}$$

TABLE 3: A Two-Parameter Fit of the Expression $k(T) = AT^n \exp(-E/RT)$[a]

n (fixed)	A ($\times 10^{-15}$ cm^3 molecule^{-1} s^{-1})	E (kJ mol^{-1})	residual sum of squares
0.5	423 ± 107	32.2 ± 1.1	117
1	10.6 ± 2.6	29.8 ± 1.1	112
1.5	0.27 ± 0.06	27.4 ± 1.0	106
2	0.007 ± 0.002	25.1 ± 1.0	101
2.5	0.00017 ± 0.00004	22.7 ± 1.0	97

[a] The value of n is fixed for the calculation of A and E. The sum of the squares of the residuals is also given.

The large standard deviations, in particular for the parameter A, show how unrealistic this parameter fitting procedure is. As already stated by Heberger et al.,[25] a three-parameter expression derived in this way might be best considered as a representation of the experimental points, which should be used only for interpolation or extrapolation of the rate coefficient values. The values of the parameters themselves have in fact no kinetic meaning. Another approach is fixing one parameter so that the fitting is reduced to a two-parameter problem. This can best be achieved by fixing the value of n on the basis of theoretical considerations followed by the calculation of the remaining two parameters.[25,26]

For a number of bimolecular rate coefficients Cohen[27] used the transition state theory to obtain a range in which the value of n is expected to vary. In the case of an atom A reacting with a molecule R−B, where R represents a complex nonlinear group and B an atom, n should lie between 0.5 and 1.5 (2.2) or between 1.0 and 2.0 (2.3) depending on the structure of the activated complex

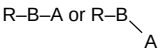

The maximum values of n between parentheses hold in cases where the anharmonicity in the new vibrations of the activated complex are taken into account. If the reaction of Cu + CH_3Cl is treated according to this formalism, the value of n probably lies between 0.5 and 2.0 (2.3). When n is fixed in the range between 0.5 and 2.5, values for the two remaining parameters A and E were now calculated with increments for n of 0.5: the results are summarized in Table 3.

One now sees that the standard deviations on the parameters A and E are much smaller than in the three-parameter fit of eq 8. It should be mentioned here that a further increase of n to, e.g., 4 resulted in a lower sum of the squares of the residuals implying a better fit, but from the viewpoint of TST, values of n above 2.3 have no fundamental meaning. When Arrhenius plots are made using the parameter sets of Table 3, the visual difference between the various plots can hardly be noticed. As an example, the curve for $n = 2$ is also shown in Figure 3. Normally, a variation in the activation barrier has a large effect on the rate constant, but in this case that effect seems to be compensated by the preexponential factor combining the parameters A and n.

To arrive at a better fit for the experimentally measured values of k_1 as a function of temperature, the following polynomial expression has been derived: $\log k_1(T) = -21.22 - 10.99(\log T) + 3.30(\log T)^2$.

Finally, it should be noticed that non-Arrhenius behaviour is also observed when different reaction channels are accessible leading to the formation of the reaction products in various electronic states. But for reaction 1, CuCl is formed in its elecronic ground state $X^1\Sigma^+$ because the exothermicity of reaction 1 of 17 kJ mol^{-1} is not enough to form the lowest

electronically excited state $A^3\Pi_2$ lying at 213 kJ mol^{-1} above the ground state.[28]

MO Calculation of the Cu−CH$_3$Cl Transition Structure. In an alternative approach to the empirical method of fixing the *n* factor, the temperature dependence of the preexponential factor could be determined on the basis of rigorous TST calculation. The rate constant can thus be expressed as[29]

$$k(T) = \kappa \frac{k_B T}{h} \frac{Q^{\ddagger}}{Q_{Cu} Q_{CH_3Cl}} \exp\left(\frac{-\Delta E^{\ddagger}_0}{RT}\right) \quad (9)$$

where κ is the transmission coefficient (for most of the reactions a value of 1 is taken for κ), k_B is the Boltzmann constant, the Q's are partition functions per unit volume and $\Delta E^{\ddagger}_0$ is the energy difference between the zero-point levels of the transition state and of the separated reactants.

From eq 9 the preexponential factor $A(T)$ can be defined as

$$A(T) = \frac{k_B T}{h} \frac{Q^{\ddagger}}{Q_{Cu} Q_{CH_3Cl}} \quad (10)$$

Combining eqs 7 and 9 one arrives at the following relation:

$$\log A(T) = \log A + n \log T \quad (11)$$

To calculate $A(T)$, one needs to know the vibrational frequencies and moments of inertia of the reactants and the transition structure. In the present study, ab initio molecular orbital calculations at the Hartree−Fock level were used to obtain vibrational frequencies and moments of inertia of CH_3Cl and the transition structure for reaction 1. Initial geometry optimization and calculation of vibrational wavenumbers at the Hartree−Fock level were performed using the Wachters basis set for Cu and a double-zeta plus polarization basis set for chlorine, carbon, and hydrogen.[30,31] Vibrational wavenumbers are scaled down by a factor 0.93 in order to reproduce a better fit with the experimental IR values of CH_3Cl. The scaled vibrational frequencies of CH_3Cl are $\nu_1 = 3054$ (1), $\nu_2 = 1408$ (1), $\nu_3 = 634$ (1), $\nu_4 = 3180$ (2), $\nu_5 = 1511$ (2), $\nu_6 = 1031$ (2) and for the transition structure they are equal to $\nu_1 = 3053$ (1), $\nu_2 = 1036$ (1), $\nu_3 = 156$ (1), $\nu_4 = 3224$ (2), $\nu_5 = 1454$ (2), $\nu_6 = 675$ (2), $\nu_7 = 75$ (2), in cm^{-1} units and with the degeneracy given in parentheses.

The moments of inertia, in units of g cm^2, are $I_A = 0.5284 \times 10^{-39}$ and $I_B = I_C = 6.7875 \times 10^{-39}$ for CH_3Cl and $I_A = 5.5997 \times 10^{-40}$ and $I_B = I_C = 5.6208 \times 10^{-38}$ for the transition structure.

The geometries of the reactants and the products were reoptimized using the quadratic configuration interaction method (QCISD). A severe convergence problem was encountered during the optimization of the transition structure at the QCISD level. Hence, a grid search was carried out as a function of both Cu−Cl and Cl−C distances at the QCISD level while keeping the other parts of the geometry fixed at their corresponding Hartree−Fock values. This resulted in the following geometry of the transition structure (C_{3v}):

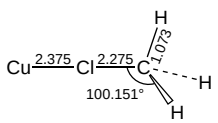

with the bond lengths expressed in Å.

Fitting the variation of the calculated value for $A(T)$ as a function of the temperature T according to eq 11 led to a slope n of 2.15 and a value A of 5.24×10^{-17} cm^3 molecule^{-1} s^{-1}. One sees that the value of n lies within the range predicted by the Cohen approach.[27] The potential energy curve for reaction 1 was then calculated by using the ab initio MO theory with the quadratic configuration interaction model (QCISD and QCISD(T)) as well as the coupled-cluster method (CCSD(T)) at QCISD geometries with the same basis set.[32] These different calculations resulted in the following barriers between the transition structure and reactants: 16.4 (QCISD), 34.4 (QCISD-(T)), and 24.8 (CCSD(T)) in kJ mol^{-1}. These values indicate on the one hand the crucial role of triple substitutions in calculating the energy barrier. On the other hand, the rather large difference between both QCISD(T) and CCSD(T) values is perplexing. Clearly, higher level calculations are needed to derive a more definitive evaluation of the energy barrier. Although the QCISD(T) estimate is closer to the experimental value derived in a previous section, we consider the CCSD(T) value as our best estimate for the energy barrier because the wave functions obtained by the coupled-cluster method are normally more elaborate then those obtained by the quadratic configuration interaction; the coupled-cluster method provides in fact a better treatment of the electron correlation. The temperature dependence of the rate constant can, using the CCSD(T) energy barrier, be expressed as

$$k_1 = 5.24 \times 10^{-17} T^{2.15} \exp\left(\frac{-24.8\ \text{kJmol}^{-1}}{RT}\right) \text{cm}^3\ \text{molecule}^{-1}\ \text{s}^{-1} \quad (12)$$

In Figure 3, expression 12 is also plotted and compared with the experimentally determined Arrhenius expression. The temperature dependence of the calculated rate constant at the CCSD(T) level follows well the three-parameter Arrhenius expression as expected from the discussion in the previous section, but the rate constant is roughly a factor 10 too high over the entire temperature range. Apparently the calculated A factor is too high or the transmission coefficient κ should be smaller than 1. Related to the same type of reaction, it has to be mentioned that in an earlier theoretical study[33] of the reaction $H + CH_3Cl \rightarrow HCl + CH_3$ a similar situation was also observed when the experimentally derived rate constants were compared with the results from TST calculation. The measured Arrhenius activation energy and the calculated energy barrier from TST are comparable, but the calculated preexponential factor is also too high by a factor of 6. An explanation for this discrepancy was also not given.

Acknowledgment. The authors are grateful to the Joint Fund for Basic Research (FKFO) for a research grant. I.V., and C.V. and M.T.N. are Research Assistant and Research Directors respectively of the National Fund for Scientific Research (NFWO), Belgium. D.S. acknowledges financial support from the Belgian Federal Government (DWTC).

References and Notes

(1) Polanyi, M. *Atomic Reactions*; Williams and Norgate Ltd.: London, 1932.
(2) Parrish, D. D.; Herm, R. R. *J. Chem. Phys.* **1971**, *54*, 2518.
(3) Weiss, P. S.; Mestdagh, J. M.; Schmidt, H.; Covinsky, M. H.; Lee, Y. T. *J. Phys. Chem.* **1991**, *95*, 3005.
(4) Herschbach, D. R. *Adv. Chem. Phys.* **1966**, *10*, 319.
(5) Ogg, R. A.; Polanyi, M. *Trans. Faraday Soc.* **1935**, *31*, 1375.
(6) Warhurst, E. *Q. Rev. Chem. Soc.* **1951**, *5*, 44.
(7) Haresnape, J. N.; Stevels, J. M.; Warhurst, E. *Trans. Faraday Soc.* **1940**, *36*, 465.
(8) Vinckier, C.; Verhaeghe, T.; Vanhees, I. *J. Chem. Soc., Faraday Trans.*, in press.
(9) Vinckier, C.; Dumoulin, A.; Corthouts, J.; De Jaegere, S. *J. Chem. Soc., Faraday Trans. 2* **1988**, *84*, 1725.

(10) Vinckier, C.; Corthouts, J.; De Jaegere, S. *J. Chem. Soc., Faraday Trans. 2* **1988**, *84*, 1951.
(11) Vinckier, C.; Verhaeghe, T.; Vanhees, I. *J. Chem. Soc., Faraday Trans*. **1994**, *90*, 2003.
(12) Vinckier, C.; Dumoulin, A.; De Jaegere, S. *J. Chem. Soc., Faraday Trans. 2* **1991**, *87*, 1075.
(13) Vinckier, C.; Christiaens, P. *J. Phys. Chem*. **1992**, *96*, 2146.
(14) Vinckier, C.; Christiaens, P. *J. Phys. Chem*. **1992**, *96*, 8423.
(15) Talcott, C. L.; Ager, J. W. III; Howard, C. J. *J. Chem. Phys*. **1986**, *84*, 6161.
(16) Fontijn, A.; Felder, W. In *Reactive Intermediates in the Gas Phase, Generation and Monitoring*; Setser, D. W., Ed.; Academic Press: New York, 1979; Chapter 2.
(17) Howard, C. J. *J. Phys. Chem*. **1979**, *83*, 3.
(18) SAS statistical package; SAS Institute Inc.; Cary, NC, 1992.
(19) Guido, M.; Balducci, G.; Gigli, G.; Spoliti, M. *J. Chem. Phys*. **1971**, *55*, 4566.
(20) Husain, D.; Marshall, P. *Int. J. Chem. Kinet*. **1986**, *18*, 83.
(21) Husain, D.; Lee, Y. H. *J. Photochem. Photobiol. A: Chem*. **1988**, *42*, 13.
(22) Husain, D.; Ji, Bing *J. Photochem. Photobiol. A: Chem*. **1989**, *48*, 1.
(23) Clay, R. S.; Husain, D. *J. Photochem. Photobiol. A: Chem*. **1991**, *56*, 1.
(24) Wu, K. T. *J. Phys. Chem*. **1979**, *83*, 1043.
(25) Heberger, K.; Kemény, S.; Vidóczy, T. *Int. J. Chem. Kinet*. **1987**, *19*, 171.
(26) Cvetanovic, R. J.; Singleton, D. L.; Paraskevopoulos, G. *J. Phys. Chem*. **1979**, *83*, 50.
(27) Cohen, N. *Int. J. Chem. Kinet*. **1989**, *21*, 909.
(28) Vinckier, C.; Corthouts, J.; De Jaegere, S. *J. Chem. Soc., Faraday Trans*. **1990**, *86*, 603.
(29) Laidler, K. J. *Chemical Kinetics*; McGraw-Hill Book Co. Inc.: New York, 1950.
(30) Wachters, A. J. H. *J. Chem. Phys*. **1970**, *52*, 1033.
(31) Dunning, T. H. *J. Chem. Phys*. **1970**, *53*, 2823.
(32) Frisch, M. J.; Trucks, G. W.; Head-Gordon, M.; Gill, P. M. W.; Wong, M. W.; Foresman, J. B.; Schlegel, H. B.; Raghavachari, K.; Robb, M. A.; Binkley, J. S.; Gonzalez, C.; Martin, R. L.; Fox, D. J.; DeFrees, D. J.; Baker, J.; Stewart, J. J. P.; Pople, J. A. *Gaussian 92*, Gaussian Inc.: Pittsburgh, 1992.
(33) Sayós, R.; Aguilar, A.; Lucas, J. M.; Solé, A.; Virgili, J. *Chem. Phys*. **1985**, *93*, 265.

JP953204O